Article ID 1004-924X(2005)05-0519-06

Design and simulation of a tuning fork micromachined gyroscope with slide film damping

CHE Lu-feng, XIONG Bin, JIAO Ji-wei, WANG Yue-lin

(*State Key Laboratory of Transducer Technology, Shanghai Institute of Microsystem and Information Technology, Chinese Academy of Sciences, Shanghai* 200050, *China*)

Abstract: A novel tuning fork micromachined gyroscope, based on slide-film damping, is presented. The electrostatic driving gyroscope consists of two driving masses each of which supports one sensitive mass. The angular rate is sensed by the differential capacitances consisted of movable bar electrodes and fixed bar electrodes located on the glass wafer. The gyroscope can operate at atmospheric pressure with slide film damping in the driving and sensing directions, eliminate vacuum packaging and restrain cross-axis acceleration signal. The results of design and simulation show that the driving and sensing mode frequencies are 3 106 Hz and 3 175 Hz, respectively, and the Q-values in driving and sensitive modes are 1 721 and 1 450 respectively. The design resolution is 0.025°/s.

Key words: micromachined gyroscope; slide film damping; design simulation

1 Introduction

Micromachined gyroscopes have attracted lots of attention during the past several years due to their small size, low cost, mass production and easy integration with electronics[1-2]. It is very improtant for aeronautics, astronautics, automobiles and military application to develop micromachined gyroscope with high performance. All vibratory gyroscopes are based on the transfer of energy between two vibration modes of a structure caused by Coriolis acceleration. A number of gyroscopes, including tuning forks, vibrating beams and vibtating shells, have been developed in past years employing different excitation and detection mechanisms. The actuation mechanisms used for driving the vibrating structure into resonance are primarily electrostatic, or electromagnetic. Electrostatic driving is implemented by electrostatic pulling force between two sets of electrodes. Electromagnetic driving[3,4] is implemented by Lorentz force, having relatively large oscillation amplitude, large driving current and complex fabrication process. To sense the Coriolis-induced vibrations in the sensing direction, capacitive, or piezoresistive detection mechanisms can be used, but for piezoresistive detection, temperature effects can be significant. So the gyroscope with electrostatic excitation and capacitive detection mechanism is the most popular. In a typical capacitive detection gyroscope where comb-type detection structure is commonly used[5], the squeeze-film damping between comb fingers plays an important role, which usually results in a low Q-factor (only 10-20) and requires costly vacuum packaging solution in some cases to achieve better sensitivity.

In our previous work[6-7], a vibratory gyroscope with slide-film damping is presented to op-

Received date: 2005-06-06; **Revised date**: 2005-06-16.

Foundation item: National natural science foundation of China project (No. 60474053)

erate at atmospheric pressure and achieve good Q-factor, but easy to be affected by cross-axis acceleration signal and cause mechanical couping because of the same mass as the driving part and sensing one. In the paper, a novel tuning fork mirogyroscope working at atmosphere with slide film damping, is presented. For the gyroscope, cross-axis acceleration signal is a common mode, while the sensing coriolis acceleration signal is a differential mode. So cross-axis acceleration signal is restrained, the sensing sensitivity is increased one time, and there is slide film damping in driving direction and sensing direction, the quality factor of the drive and sense are about 1 000 at atmosphere and the sensitivity is greatly increased, which eliminates vacuum packaging and reduces packaging difficulties and manufacturing cost.

2 Structure and principle

As shown schematically in Fig. 1, the gyroscope consists of two symmetrical parts, each of which consists of a driving mass and a sensing one, and is anchored on glass substrate by four spring beams and is connected each other through a connection spring. Each sensing mass with bar structure detection electrodes is connected by two suspension beams to the surrounding driving mass with bar structure driving electrodes. There are fixed bar driving electrodes and sensing electrodes on glass substrate under corresponding movable bar electrodes, respectively.

The driving mass as well as the sensing mass with bar structure can move above the glass substrate along X or Y direction. When AC and DC voltages are applied between driving bar electrodes, electrostatic force generated drives the two driving masses to vibrate out-of-phase mode along X-direction. If an angular rate vertical to substrate is applied, two sensing masses will oscillate out-of-phase mode along Y di-

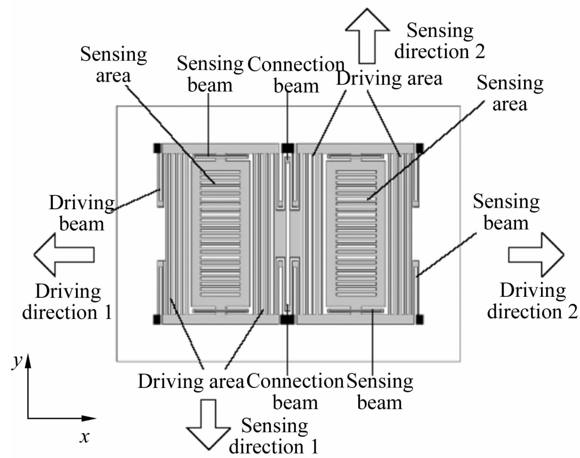

Fig. 1 Structure of the gyroscope

rection due to Coriolis force. The resulting capacitance change between bar structure sensing electrodes and fixed ones can be sensed differentially, accordingly the angular rate is measured and Y-direction acceleration cancels out meanwhile.

The gyroscope is actuated electrostatically by a push-pull driving circuit as shown in Fig. 2.

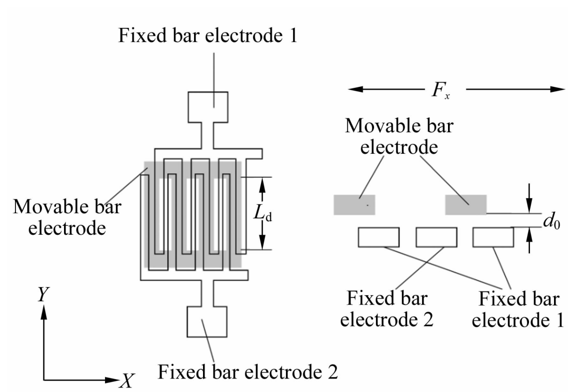

Fig. 2 Structure of the driving part

The driving voltages on the fixed electrodes 1, V_1, and the fixed ones 2, V_2, are $V_1 = V_0 + V_d \sin(\omega t)$ and $V_2 = V_0 - V_d \sin(\omega t)$, respectively. The resulting driving force (tangential force) F_x is

$$F_x = \frac{1}{2}\frac{\partial C}{\partial x}V_1^2 - \frac{1}{2}\frac{\partial C}{\partial x}V_2^2 , \tag{1}$$

The driving capacitance C is defined by

$$C=\frac{N_d \varepsilon L_d x}{d_0} \quad , \tag{2}$$

where N_d is the number of driving electrodes, ε is the dielectric constant in air, L_d and x are the effective overlapping length and width of driving electrodes, respectively, and d_0 is the distance between the movable electrodes and the fixed electrodes.

Considering equations (1) and (2), the driving forces become

$$F_x=\frac{N_d \varepsilon L_d}{2d_0}(V_1^2-V_2^2)=\frac{2N_d \varepsilon L_d}{d_0}V_0 V_d \sin(\omega t) \quad , \tag{3}$$

The movable bar sensing electrodes and the fixed interdigitated ones form detection capacitances C_1 and C_2 as shown in Fig. 3. When the bar has a displacement y along Y-direction due to Coriolis force, neglecting the fringe effects of the electrical field, capacitances C_1 and C_2 are defined by

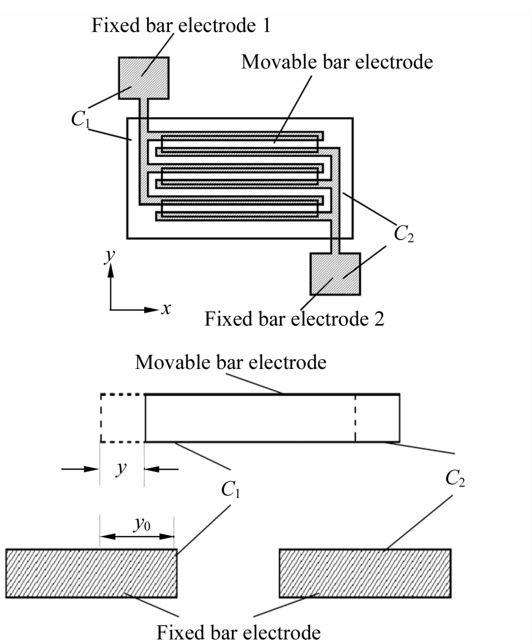

Fig. 3 Structure of the sensing part

$$C_1=\frac{A_y}{2}(y_0-y) \quad , \tag{4}$$

$$C_2=\frac{A_y}{2}(y_0+y) \quad . \tag{5}$$

The differential capacitance change is

$$\Delta C=C_2-C_1=2C_0 \frac{y}{y_0} \quad , \tag{6}$$

Where $A_y=2N_s \varepsilon L_s/d_0$, y is the oscillation displacement of the sensing mode, N_s is the number of detection electrodes, L_s is the effective overlapping length of sensing electrodes, and y_0 is the effective overlapping width of sensing electrodes, d_0 is the gap between interdigitated electrodes and bar structure, C_0 is the stationary capacitance of C_1 and C_2.

When an angular rate is applied, two sets of movable sensing electrodes vibrate out-of-phase mode. If cross-axis acceleration signal is inputted, two sets of movable sensing electrodes vibrate in phase mode. So cross-axis acceleration signal is restrained and the sensing sensitivity is increased one time by two sets of differential capacitance change.

In the gyroscope, both driving mass and sensing mass are designed to move parallel to the glass substrate. In the air gaps between movable bar electrodes and fixed bar electrode as driving and sensing, the dominant air damping is slide-film damping. Compared with the squeeze-film damping, the slide-film damping is much smaller and thus high Q factors are ensured for both driving and sensing modes even at atmospheric pressure.

The resonant frequencies of the driving and sensing mode designed are relatively low, so we can use Couette-type model to calculate the slide film damping[8], the damping coefficient is

$$c=\frac{\mu A}{h} \quad , \tag{7}$$

where μ is the absolute viscosity of air, A is the area of the moving mass, h is the gap between the movable mass and substrate.

3 System modeling and performance analysis

3.1 Model of driving system

The two driving masses of the gyroscope resemble as a tuning fork. The major advantages of a tuning fork are the stable center of gravity and the compensation of all forces and moments of inertia within the chip. This tuning fork type gyroscope is electrostatically driven out of phase

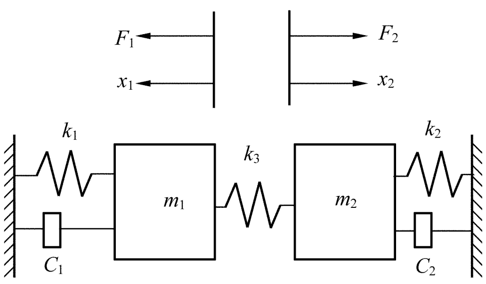

Fig. 4 Model of the driving system

mode. The driving system can be simplified as a spring-mass-damping system with two spring-coupled masses as shown in Fig. 4. The basic equations of the driving motion of the gyroscope are given by

$$m_1\ddot{x}_1+c_1\dot{x}_1+(k_1+k_3)x_1+k_3x_2=F_1 \quad , (8)$$

$$m_2\ddot{x}_2+c_2\dot{x}_2+k_3x_1+(k_2+k_3)x_2=F_2 \quad . (9)$$

where m_1 and m_2 are driving masses, k_1 and k_2 is the driving spring constants, c_1 and c_2 are the damping coefficients in the driving direction, k_3 is the coupling spring constant connecting two driving masses, F_1 and F_2 are driving forces out of phase. Considering structure design , these conditions are met: $m_1=m_2=m$, $c_1=c_2=c$, $k_1=k_2=k$, $F_1=F_2=F=F_0\sin(\omega t)$.

The driving system has two natural oscillating modes: in phase and out of phase, the resonant frequency can be expressed as:

$$\omega_1=\sqrt{\frac{k}{m}} \quad \text{(in phase)}, \qquad (10)$$

$$\omega_2=\sqrt{\frac{k+2k_3}{m}} \quad \text{(out of phase)}. \qquad (11)$$

According to equation (8) and (9), the steady amplitude of driving oscillation out of phase is:

$$B_d=\frac{F_0}{(k+2k_3)\sqrt{(1-\lambda_d^2)^2+4\xi_d^2\lambda_d^2}} \quad , \qquad (12)$$

where $\xi_d=\frac{c}{2m\omega_2}, \lambda_d=\frac{\omega}{\omega_2}$

3.2 Performance analysis and simulation

For the tuning fork gyroscope, its work mode is out of phase one i. e. , two driving masses vibrate in opposite direction. In order to cancel the coupling between in phase mode and out of phase mode, the system is optimized to separate the resonant frequency of out of phase mode from in phase mode. The coupling spring k_3 mainly affects the frequency difference of in phase mode and out of phase one.

For diminishing the effect of environmental noise (<2 kHz), the resonant frequency for driving mode is chosen as 3 106 Hz, while the resonant frequency for sensing mode is chosen as 3 175 Hz. The driving mode and sensing mode of the gyroscope simulated by ANSYS are shown in Fig. 5. The calculated results show that the Q-factors for driving and sensing modes at each resonant frequency are 1 721 and 1 450, respectively.

Under the effect of driving force ($F=F_0\sin(\omega t)$), applying an angular rate Ω vertically on the substrate, the basic equation of sensing motion of the gyroscope is given by

$$m_s\ddot{y}+c_s\dot{y}+k_s y=2m_s\Omega\dot{x}_1\ , \tag{13}$$

where m_s is the sensing mass, c_s is damping coefficient of sensing mode, k_s is spring constant of sensing mode.

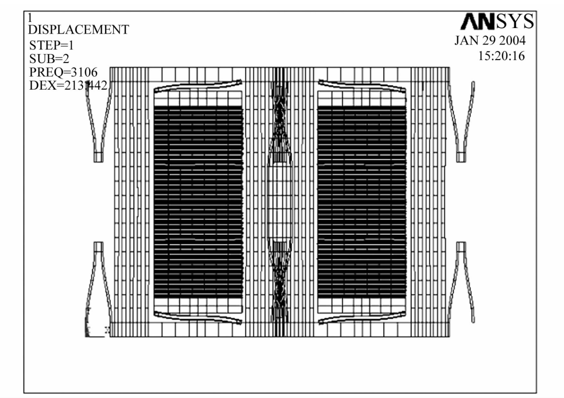

(a) Driving oscillation mode

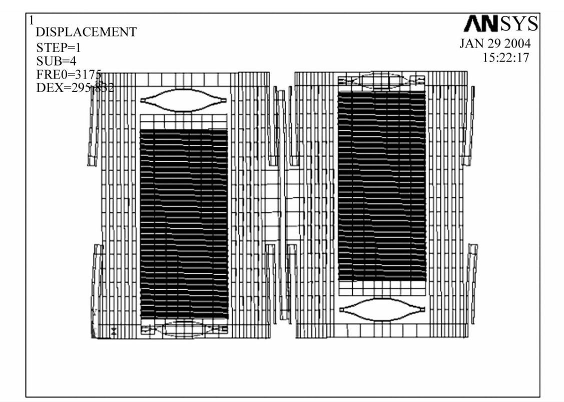

(b) Sensing oscillation mode

Fig. 5 Mode shape of the gyroscope

The steady amplitude of driving oscillation is defined by equation (12), so the steady amplitude of sensing oscillation is:

$$B_s=\frac{2\Omega B_d\omega m_s}{k_s}\frac{1}{\sqrt{(1-\lambda_s^2)^2+4\xi_s^2\lambda_s^2}}\ , \tag{14}$$

where $\omega_s^2=\frac{k_s}{m_s}$, $\xi_s=\frac{c_s}{2m_s\omega_s}$, $\lambda_s=\frac{\omega}{\omega_s}$

According to equation (3)、(7) and (14), the steady change of sensing capacitance is

$$\Delta C=\frac{8C_0\Omega B_d m_s\omega}{y_0 k_s}\frac{1}{\sqrt{(1-\lambda_s^2)^2+4\xi_s^2\lambda_s^2}}\ , \tag{15}$$

For driving voltage 5 V AC and 10 V DC, angular rate Ω 1°/s(0.017 rad/s), frequency response of sensing oscillation amplitude is shown in Fig. 6. The curve has two peak values at driving mode frequency point and sensing mode frequency point. When driving frequency is equal to driving mode frequency 3 106 Hz, according to equation (15), the change of sensing capacitance is 386.7aF. When the resolution of sensing circuit is 10 aF, the design resolution of the gyroscope is 0.025 °/s.

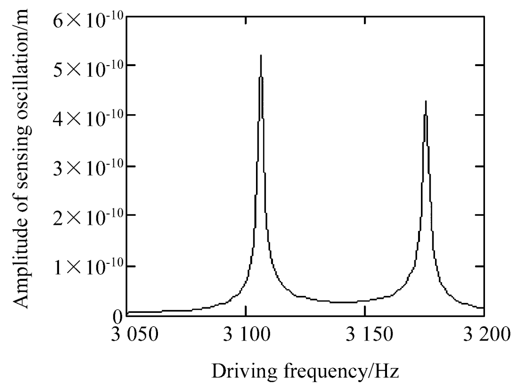

Fig. 6 Frequency response of sensing oscillation amplitude

4 Summary

A novel tuning fork micromachined gyroscope is presented, which has independent folded beam and reduces mechanical coupling. The gyroscope can restrain cross-axis acceleration signal, operate at atmospheric pressure with slide film damping in the driving and sensing directions and eliminate vacuum packaging. The design resolution of the gyroscope is 0.025°/s. The gyroscope is in fabrication and maybe has relatively good performance.

References:

[1] YAZDI N, AYAZI F, NAJAFI K. Micromachined inertial sensors[J]. *Proceedings of the IEEE*, 1998, 86(8): 1640-1659.

[2] MOCHIDA Y, TAMURA M, OHWADA K. A micromachined vibrating rate gyroscope with independent beams for the drive and detection modes[J]. *Sensors and Actuators A*, 2000, 80(2): 170-178.

[3] LUTZ M , GOLDERER W, GERSTENMEIER J, *et al*. A precision paw rate sensor in silicon micromachining [C]. *Transducers'97*. *Chicago*, 1997:847-850.

[4] HASHIMOTOT M, CABUZ C, MINAMI K, *et al*. Silicon resonant angular rate sensor using electromagnetic excitation and capacitive detection[J]. *Journal of Micromechanics and Microengineering*, 1995, 5(3):219-225.

[5] BERNSTEIN J, CHO S, KING A T, *et al*. A micromachined comb-drive tuning fork rate gyroscope[C]. *Proc. IEEE Micro Electro Mechanical Systems Workshop* (*MEMS'93*). *Fort Lauderdale*, 1993:143-148.

[6] CHE L F , XIONG B , WANG Y L . System modelling of a vibratory micromachined gyroscope with bar structure [J]. *Journal of Micromechanics and Microengineering*, 2003, 13(1):65-71.

[7] XIONG B, CHE L F, WANG Y L. A novel bulk micromachined gyroscope with slots structure working at atmosphere[J]. *Sensors and Actuators A*, 2003, 107(2): 137-145.

[8] BAO M H. *Micro mechanical transducers pressure sensors, accelerometers and gyroscopes*[M]. Amsterdam: Elsevier Press, 2000.

Brief professional biographies of the authors:

CHE Lu-feng obtained his PhD degree in mechnical engineering from Zhejiang University in 1999. From 1999 to 2001, he was a post-doc at State Key Laboratory of Transducer Technology, Shanghai Institute of Microsystem and Information Technology(SIMIT), Chinese Academy of Sciences(CAS). He is a visiting scholar at University of California at Berkeley in 2005. He is an associate professor of SIMIT. His research interests include design, fabrication, testing and system integration of MEMS sensors and actuators.

XIONG Bin received his BS degree from Southeast University in 1984, MS degree and PhD degree from Shanghai Institute of Microsystem and Information Technology(SIMIT), Chinese Academy of Sciences(CAS), in 1997 and 2001, respectively. Now he is a professor in SIMIT. His current research interests include sensors, MEMS and related technology.

JIAO Ji-wei received his BS degree from Zhejiang University in 1989, PhD degree from Shanghai Institute of Microsystem and Information Technology(SIMIT), Chinese Academy of Sciences(CAS), in 1994, respectively. Now he is a professor in SIMIT. His current research interests include sensors, MEMS and related technology.

WANG Yue-lin received his BS, MS and degrees from Zhejiang University, Harbin Institute of Technology and Tsinghua University, China, in 1982, 1985 and 1989, respectively. Since 1993 he was been a professor at Zhejiang University and Shanghai Institute of Microsystem and Information Technology(SIMIT), Chinese Academy of Sciences(CAS). His current research interests include sensors, MEMS and related technology.